Title: Hydrogen Sulfide Oxidation by Sulfide Quinone Oxidoreductase

Authors: Aaron P. Landry; David P. Ballou; Ruma Banerjee

To be cited as: 10.1002/cbic.202000661

Link to VoR: https://doi.org/10.1002/cbic.202000661

Hydrogen Sulfide Oxidation by Sulfide Quinone Oxidoreductase

Aaron P. Landry, David P. Ballou, and Ruma Banerjee*

Department of Biological Chemistry, University of Michigan Medical School, Ann Arbor, Michigan 48109, United States

*Corresponding Author: rbanerje@umich.edu

Abstract

Hydrogen sulfide (H_2S) is an environmental toxin and a heritage of ancient microbial metabolism, which has stimulated new interest following its discovery as a neuromodulator. While many physiological responses have been attributed to low H_2S levels, higher levels inhibit complex IV in the electron transport chain. To prevent respiratory poisoning, a dedicated set of enzymes comprising the mitochondrial sulfide oxidation pathway exists to clear H_2S. The committed step in this pathway is catalyzed by sulfide quinone oxidoreductase (SQOR), which couples sulfide oxidation to coenzyme Q_{10} reduction in the electron transport chain. The SQOR reaction prevents H_2S accumulation and generates highly reactive persulfide species as products, which can be further oxidized or can modify cysteine residues in proteins via persulfidation. Here, we review the kinetic and structural characteristics of human SQOR, and how its unconventional redox cofactor configuration and substrate promiscuity lead to sulfide clearance and potentially expand the signaling potential of H_2S. This dual role of SQOR makes it a promising target for H_2S-based therapeutics.

Introduction

Hydrogen sulfide (H_2S) is a volatile, flammable, and toxic gas, with a characteristic odor of rotten eggs that is detectable by the human nose at levels as low as 0.02-0.03 ppm.[1-2] The primary mechanism of H_2S toxicity is via tight binding to heme a_3 in cytochrome *c* oxidase, inhibiting mitochondrial respiration.[3] Owing to its toxicity, H_2S has long been infamous as an occupational and environmental hazard,[1-2, 4] but its reputation underwent a paradigm shift in 1996 with the discovery of its neuromodulatory role.[5] Since its induction into the family of gaseous signaling molecules along with nitric oxide (NO) and carbon monoxide (CO), significant strides have been made in understanding the physiological effects of H_2S, which span the cardiovascular, central nervous, and gastrointestinal systems.[6]

To elicit signaling responses, cellular H_2S levels presumably increase sharply, before returning to low steady-state levels to prevent respiratory poisoning.[7] Alternatively, H_2S-based signaling might originate from transient inhibition of mitochondrial bioenergetics, which is reversed by the action of SQOR.[8] Physiological effects in response to H_2S typically display a bimodal response that is dependent on the concentration of H_2S. High H_2S levels have been implicated in peripheral and coronary artery diseases,[9] stimulation of the growth and plasticity of colon, liver, and breast cancers,[10-11] septic shock,[12] and inflammation,[13-14] while low H_2S levels are implicated in hypertension,[15] acceleration of atherosclerosis,[16] and fibrotic disease in several organs.[17-18] Intriguingly, H_2S has been reported to reversibly induce a state of suspended animation in mice.[19] The multitude of disease correlations have led to a growing interest in H_2S-based therapeutics.[20-21]

While the physiological effects of H_2S have been extensively studied, the mechanism by which these effects are elicited are still in the early stages of investigation. Unlike NO and CO,[22-23] H_2S does not have a known second messenger that transduces its signal. A prevailing hypothesis for H_2S-mediated signaling is that it involves protein persulfidation, which leads to the reversible modification of cysteine residues.[24-25] Under physiological conditions, H_2S (pK_a = 6.76 at 37 °C) exists predominantly as the nucleophilic sulfide anion (HS^-),[26] which can react with oxidized cysteines such as S-glutathionyl, S-nitrosyl, or sulfenyl species forming the corresponding persulfide (Figure 1A).[27] Alternatively, reduced cysteines can be persulfidated by a low molecular weight persulfide (RSSH)[27] or in a reaction catalyzed by a sulfurtransferase (Figure 1B).[28] Not surprisingly, the number of persulfidated proteins in cells increases upon H_2S treatment.[29] The association between protein persulfidation and the modulation of protein function in several biochemical processes has been reviewed previously.[27, 30-31] This review focuses on sulfide quinone oxidoreductase (SQOR), which catalyzes the first and committing step in the mitochondrial sulfide oxidation pathway, and could serve as the "off-switch" in H_2S-based signaling or the "on-switch" in persulfide based signaling, or both. SQOR is a mitochondrial inner membrane-anchored flavoenzyme that is poised to play a critical role in H_2S-based signaling while also serving as a guardian of the electron transfer chain against H_2S poisoning.[8]

1. H_2S biogenesis and catabolism

1.1. Enzymatic / microbial H_2S production

Endogenous production of H_2S can be catalyzed by at least three enzymes of which two are in the transsulfuration pathway, linking the methionine cycle to cysteine and glutathione (GSH) synthesis (Figure 2A).[32-33] Cystathionine β-synthase (CBS), the first enzyme in this pathway, produces H_2S primarily via condensation of cysteine and homocysteine,[34] while cystathionine γ-lyase (CSE), the second enzyme in the pathway, produces H_2S primarily via α, β-elimination of cysteine, forming pyruvate and ammonia in the process.[35] The relative contributions of CBS and CSE to H_2S production can be estimated based on their tissue-specific expression levels, their reaction velocities, and the physiological concentrations of their substrates.[36-37] The third H_2S-synthesizing enzyme, 3-mercaptopyruvate sulfurtransferase (MPST), is involved in cysteine catabolism and initially produces an enzyme-bound persulfide via the desulfuration of 3-mercaptopyruvate.[38] The final persulfide product can be a low molecular weight species (e.g. cysteine persulfide) or is protein bound (e.g. on thioredoxin), and can release H_2S in the presence of a reductant, or transfer sulfane sulfur to an acceptor.[39] The two MPST isoforms in the cytoplasm (MPST1) and in the mitochondrion (MPST2), have nearly identical kinetic profiles, but differ in their tissue expression levels.[39] The steady-state H_2S concentration in mammalian cells and tissues is estimated to range from 10–30 nM.[7, 40-41] An interesting exception is the aorta, in which significantly higher H_2S levels are reported (~1.8 μM), potentially related to a role for H_2S in vasodilation.[41]

In contrast to most cells, colonocytes, which line the colonic lumen, are exposed to high H_2S concentrations derived from microbial metabolism that are reported to range from 0.2-2.4 mM.[42-43] The gut microbial population is vast and is estimated to comprise 10-100 trillion organisms,[44] including sulfate-reducing bacteria.[45] Since H_2S can freely diffuse across membranes,[46] it potentially exposes the colonic epithelium to toxic levels of this gas. Hence, to prevent respiratory poisoning, colonocytes must be adapted to withstand acute or steady exposure to high levels of H_2S. The colonic epithelium is protected from invasive microbial growth by a two-layer barrier of mucus,[47] which is enriched with glycoproteins secreted by goblet cells.[48] However, it is largely unknown whether this protection extends to H_2S entry. On the other hand, defective H_2S clearance in colonocytes has been implicated in ulcerative colitis, which is marked by decreased butyrate oxidation[49-50] that, as discussed below, is an important source of energy for these cells.

1.2. Overview of the mitochondrial sulfide oxidation pathway

In mammals, the sulfide oxidation pathway resides in the mitochondrion and begins with SQOR (Figure 2B). The SQOR reaction couples H_2S oxidation to coenzyme Q_{10} (CoQ) reduction.[51-54] Under physiological conditions, the primary sulfane sulfur acceptor for the SQOR reaction is GSH, generating glutathione persulfide (GSSH) as the product.[53-54] GSSH is then further oxidized by the iron-dependent persulfide dioxygenase, ETHE1, to produce sulfite and regenerate GSH.[55-56] GSSH is also a substrate for rhodanese (or TST), a sulfurtransferase that catalyzes the reaction of GSSH with sulfite to produce GSH and thiosulfate.[53, 57] Alternatively,

sulfite is oxidized to sulfate by sulfite oxidase, which resides in the intermembrane space.[58] Electrons from the sulfide oxidation pathway enter the electron transfer chain at the level of Complex III (from SQOR) and cytochrome *c*/Complex IV (from sulfite oxidase).

The end products of the pathway, thiosulfate and sulfate, can be excreted. In serum, thiosulfate levels of ~0.6 μM[59] and significantly higher sulfate levels (~300 μM) have been reported.[60] Thiosulfate and sulfate concentrations are higher in urine at ~9 μM[61] and ~17 mM,[62] respectively. In sulfite oxidase deficiency thiosulfate levels increase dramatically and have been reported to be ~2 mM.[62] Thiosulfate levels in the blood and urine also increase after acute H_2S exposure, thus serving as a biomarker of H_2S poisoning.[63-64]

2. SQOR belongs to the flavin disulfide reductase superfamily

2.1. Flavin disulfide reductases

SQOR is a member of the diverse and extensive flavin disulfide reductase (FDR) superfamily.[65-66] FDRs often share a common mechanistic characteristic in which the flavin and the disulfide transfer electrons to one another via a transient covalent flavin C4a-S-Cys adduct. FDRs each have a tightly bound flavin cofactor, most often FAD, along with a cysteine-based center. In most instances, the flavin mediates electron transfer between thiol-disulfide exchange reactions at the cysteine-based center and organic redox molecules, including the pyridine nucleotides NADP(H) or NAD(H), quinones such as CoQ, or cytochrome *c*. A reduced cysteine-based center can transfer electrons to oxidized substrates including glutathione disulfide and lipoamide; alternatively, substrates including sulfide can drive electrons to an active site cysteine disulfide, which are then relayed to the flavin. A catalytic triad (Glu-His-Cys) that stabilizes the thiolate nucleophile is frequently, but not always, found in the active site of these enzymes.

The so-called classical Group 1 FDRs are typified by glutathione reductase, lipoyl dehydrogenase, and trypanothione reductase.[65-66] Group 2 also has the classical fold, but with an additional dithiol containing domain and include the high molecular weight form of thioredoxin reductase, mercuric reductase, and thioredoxin glutathione reductase. Group 1 and 2 FDRs are most often obligate homodimers because FAD, pyridine nucleotide, and cysteine domains are in one subunit, while the active site base including the catalytic triad is from another. In addition, both the binding and specificity of the non-pyridine nucleotide substrate are often contributed by both monomers.

Group 3 FDRs, including NADH peroxidase, do not contain a di-cysteine center, but instead, a single cysteine that undergoes 2-electron oxidation by H_2O_2 to sulfenic acid. The cysteine can form a charge transfer (CT) complex with the flavin, as seen with other enzymes in the FDR superfamily. NADH reduces the flavin, which transfers electrons to the sulfenic acid, eliminating H_2O.[67] CoA disulfide reductase has a similar single cysteinyl center, which undergoes a thiol-disulfide exchange with CoA disulfide. This exchange releases one CoASH and concomitantly forms a covalent CoA disulfide with the active site cysteinyl residue. The Cys-S-S-CoA mixed disulfide is then reduced by NADPH via the flavin, releasing CoASH.[68]

Group 4 FDRs, which includes SQOR, is the most diverse both structurally and functionally. SQORs contain two redox active cysteines that are widely separated in the primary sequence but are spatially proximal.[69-73] A hallmark of this subgroup is that they can utilize diverse substrates. Many members, including SQOR and flavocytochrome *c* sulfide dehydrogenase (FCSD), do not use pyridine nucleotides, but instead, substitute CoQ (in SQOR), or cytochrome *c* (in FCSD) as an electron acceptor. In both of these cases, the enzymes oxidize sulfide. SQOR utilizes several of the chemical principles common to the FDR superfamily, as well as some unique sulfur-based chemistry during the catalytic cycle.

2.2. Classification of SQORs

SQORs are broadly distributed across all domains of life, owing to their pleiotropic roles spanning sulfide oxidation-driven energy production in bacteria and archaea to conveying sulfide tolerance to higher organisms. Following initial attempts to classify SQORs based on sequence data,[74-75] a clearer picture emerged as the first SQOR structures became available for the archaeal *Acidianus ambivalens*[70] and the bacterial *Aquifex aeolicus*[69] and *Acidithiobacillus ferrooxidans*[71] proteins. While the structures were similar overall, significant differences were seen in the FAD binding mode, the channel for active site access to sulfide, and the configuration of active site residues. Structure and function-based sequence fingerprints were used to classify SQORs into six groups.[76-77] Among these, the Type II SQORs encompass SQORs from all eukaryotes, including the human enzyme as well as SQOR from α-proteobacteria.

Mechanistically, Type II SQORs are more similar to FCSDs than to other SQOR types.[76] FCSDs are found exclusively in bacteria that live in sulfide-rich environments,[77] and couple H_2S oxidation in the flavin-containing subunit to heme reduction in a separate cytochrome *c* subunit.[78] The FCSD reaction requires a cysteine disulfide, FAD, and a second equivalent of H_2S as an acceptor, producing hydrodisulfide (HSSH). While FCSD and SQOR both contribute to energy production by driving sulfide-derived electrons into the respiratory chain, the SQOR reaction is more efficient since it enters earlier, at the level of complex III rather than IV, resulting in more protons being pumped and more ATP being generated. The purple sulfur bacterium *Allochromatium vinosum*, which possesses both FCSD and SQOR, preferentially uses the latter for sulfide oxidation, consistent with the higher energy yield from SQOR.[79-80]

3. Enzymology of human SQOR

3.1. Sulfide oxidation is coupled to CoQ reduction

The first structures of SQOR were reported a decade ago and were from bacteria.[69-71] The first structures of human SQOR were reported only recently,[72-73] and provided unexpected insights into the catalytic mechanism, as discussed later. Human SQOR is structurally similar to the *Acidithiobacillus ferrooxidans* SQOR (Figure 3A)[71] and to the flavoprotein subunit of FCSD (Figure 3B).[78] In each case, two tandem Rossmann folds harbor the FAD cofactor and two amphipathic helices at the C-terminus anchor the enzyme to the membrane. The redox-active cysteinyl residues in human SQOR, ^{379}Cys and ^{201}Cys, reside on the *re* face of FAD, and

surprisingly, exist in a trisulfide configuration bridged by an additional sulfane sulfur atom (Figure 3C).[72-73] The *si* face of the FAD faces the CoQ binding pocket, which leads to the protein surface via a hydrophobic tunnel that presumably facilitates the movement of the hydrophobic CoQ between the active site and the lipid bilayer. Unlike the bacterial enzymes in which the active site appears to be protected from solvent, a large cavity on the surface of human SQOR leads to the active site and partially exposes ^{379}Cys to the bulk solvent of the mitochondrial matrix (Figure 3C).

SQOR-catalyzed oxidation of H_2S proceeds via two half reactions (Figure 4). The oxidative half reaction is initiated upon sulfide addition to the cysteine trisulfide, presumably by nucleophilic attack on the more exposed ^{379}Cys. Of the resulting pair of persulfides,^{379}Cys-SSH is surface exposed while ^{201}Cys-SSH is engaged in an unusually intense charge transfer (CT) interaction with the FAD cofactor, exhibiting an absorbance maximum at 675 nm with an absorbance coefficient of ~8 mM^{-1} cm^{-1}.[52, 54, 73, 81] The first half reaction is completed upon transfer of the sulfane sulfur from ^{379}Cys-SSH to a small thiophilic acceptor, e.g. GSH, regenerating the cysteine trisulfide and leading to the two-electron reduction of FAD, presumably via the transient formation of a C4a adduct with the persulfide of ^{201}Cys. The second half reaction then proceeds through electron transfer from $FADH_2$ to CoQ, regenerating the resting enzyme. Reduced CoQ enters the electron transport chain at the level of complex III, making sulfide the first known inorganic substrate for human mitochondrial energy production.[82]

3.2. A cysteine trisulfide is the redox-active motif in human SQOR

An unexpected surprise revealed by the crystal structures of human SQOR was that the redox active cysteines are ~4 Å apart, precluding formation of a direct disulfide bond in the absence of a large conformational change.[72-73] Instead, the two cysteines were linked via a bridging sulfur atom (Figure 3C), which was confirmed via sulfur anomalous diffraction analysis.[73] This configuration contrasts with that of other members of the FDR superfamily, in which the redox active cysteines exist as a disulfide in the oxidized state. The cysteine trisulfide configuration was initially ascribed as a purification artifact and was postulated to represent an inactive form of the enzyme.[72] A chemically unusual mechanism was proposed to explain how the trisulfide converted to a cysteine disulfide, involving Cβ-S bond cleavage in one of the cysteines and the mechanism by which the distance between the cysteines would be bridged was not addressed.[72] In contrast, studies in our laboratory led to the conclusion that the trisulfide represents the active form of SQOR, and it is reformed at the end of catalytic turnover.[73] To our knowledge, human SQOR is the first reported example of an enzyme in which the catalytically active redox cofactor has a cysteine trisulfide configuration. It is possible that the bacterial homologs have a similar configuration, although resting enzyme structures are not available. Instead, crystal structures have captured active site configurations with Cys-S-SSS-S-Cys[70, 83] and cyclooctasulfur-bound (Cys-S-S_8) intermediates.[69] Cysteine trisulfides have been observed previously, e.g., as an artifact in recombinant human growth hormone.[84-87] They have also been proposed as intermediates in the catalytic cycle of *Aquifex aeolicus* SQOR, which generates polysulfide rather than a persulfide product,[69] and in the catalytic cycle of the bacterial dissimilatory sulfite reductase DsrC.[88]

The bridging sulfur in the human SQOR cysteine trisulfide is sensitive to cyanolysis, which was initially used to detect its presence biochemically.[73] Cyanolysis was shown to occur via nucleophilic addition of the cyanide to the trisulfide, forming a transient CT complex.[89] Subsequent decay of the CT complex leads to a disulfanyl-methanimido thioate intermediate, which was trapped *in crystallo*. The bridging sulfur is extracted from this intermediate in the presence of excess cyanide, preserving the oxidation state of the active site cysteines as a cyclized ^{201}Cys-S-N=CHS-^{379}Cys species in an inactive form of the enzyme.[89] Incubation of cyanide-treated SQOR with sulfide reforms the resting trisulfide, reactivating the enzyme. These analyses provided insights into how the trisulfide might be initially built in human SQOR, which is currently under investigation in our laboratory.

Minimally, two mechanisms can be considered for trisulfide formation. In the first, both cysteines are oxidized (e.g., to cysteine sulfenic acid), followed by the attack of a sulfide anion to form a persulfide (e.g., on the solvent accessible ^{379}Cys (Figure 5A, *1* → *3*). Then, attack of the ^{379}Cys-SSH on the sulfenic acid moiety of ^{201}Cys generates the trisulfide. In the second mechanism, both cysteines undergo persulfidation, an oxidative cysteine modification that has been detected in many proteins.[29] Low molecular weight persulfides (e.g. cysteine persulfide) could lead to the formation of a bis-persulfide intermediate (Figure 5B, *1* → *2*) from which the trisulfide could be built. Low molecular weight persulfides are synthesized by all three H_2S generating enzymes,[38-39, 90-91] and a potential role for these reactive sulfur species in signaling has been proposed.[27] Alternatively, generation of the trisulfide in SQOR could be catalyzed via sulfur transfer from a protein-bound persulfide. Candidate human sulfur transferases include rhodanese,[57] MPST,[38] and TSTD1.[28] We note that these two mechanisms could coexist. The cysteine trisulfide is more reactive than a cysteine disulfide both in terms of electrophilicity and leaving group potential. Computational modeling and molecular dynamics simulations estimate that the trisulfide configuration contributes an ~10^5-fold rate enhancement over a disulfide for the initial nucleophilic addition of sulfide,[89] accounting for much of the ~10^7-fold higher rate constant for sulfide addition to SQOR versus to a cysteine disulfide in solution.[92]

3.3. Substrate promiscuity leads to dead-end complexes

Human SQOR exhibits remarkable substrate promiscuity, and in addition to sulfide, a number of nucleophiles can add to the resting trisulfide. Thus, in addition to sulfide (k_{on} = 4 × 10^6 $M^{-1}s^{-1}$ at 4 °C),[54] other nucleophiles add to the trisulfide with rate constants that range over 10^5-fold under the same assay conditions, including sulfite (940 $M^{-1}s^{-1}$), GSH (0.38 $M^{-1}s^{-1}$), methanethiol (6.3 × 10^4 $M^{-1}s^{-1}$), and CoA.[73, 81, 93] The addition of alternative nucleophiles to resting SQOR leads to the corresponding ^{379}Cys mixed disulfide and the ^{201}Cys-SS^- persulfide that forms an intense CT complex with FAD. Unlike the sulfide-induced CT complex, which decays quickly to yield $FADH_2$,[52, 81] the alternative CT complexes represent dead-end complexes and decay slowly at rates that approximate the respective dissociation rate constants (k_{off}) for the nucleophiles (Figure 6A).[93] Although these dead-end complexes could entrap SQOR in an unproductive state, their formation is suppressed to some extent by the membrane environment of SQOR, as revealed

by a comparative kinetic analysis of the solubilized versus nanodisc-embedded protein.[93] Under certain pathological conditions, however, such as sulfite oxidase deficiency that is marked by elevated sulfite,[94] oxidative stress conditions that lead to GSH depletion,[95-96] or periodontitis marked by elevated methanethiol,[97-98] adventitious nucleophilic additions into the active site trisulfide in SQOR could become physiologically relevant and lead to impaired H_2S clearance.

The CT complex formed upon addition of sulfide or an alternative nucleophile has an unusually large absorbance coefficient (Figure 6A) relative to those of thiolate-to-FAD CT complexes observed in other FDRs,[99-103] including the structurally related FCSD.[104] The electron-rich persulfide-to-FAD interaction in SQOR that was predicted to form from the resting trisulfide has been captured crystallographically (Figure 6B),[73] revealing the structural basis for the unusual intensity of the CT complex. The CT complex in SQOR is reminiscent of the robust CT complex seen in short-chain acyl-CoA dehydrogenase (ACADS), which is formed between a tightly-bound CoA persulfide and FAD (Figure 6C).[105]

3.4. SQOR accommodates alternate sulfane sulfur acceptors

The substrate promiscuity of human SQOR also extends to the sulfur transfer step to a low molecular weight thiophilic acceptor, and potentially leads to a variety of reactive sulfur species as products (Figure 7). Identifying the physiologically relevant sulfane sulfur acceptor is germane to understanding the logic of how the sulfide oxidation pathway is organized. The two major proposals for the physiologically relevant acceptor are sulfite, which leads to thiosulfate formation[52] and GSH, which leads to GSSH formation.[53]

The proposal that sulfite is the primary physiological acceptor was largely based on *in vitro* kinetic data. The k_{cat}/K_M for sulfite is ~2×10^6 $M^{-1}s^{-1}$,[52-54] and thiosulfate production was observed during sulfide oxidation in lugworm and rat liver mitochondria,[51] and in colon.[106] In this model, thiosulfate is postulated to be an intermediate in the production of sulfate,[107-108] which would require the kinetically unfavorable conversion of thiosulfate to GSSH via the rhodanese-catalyzed sulfur transfer reaction,[53] followed by oxidation of GSSH by ETHE1 to sulfite[55] for use by the SQOR catalytic cycle. However, this model is inconsistent with the very low intracellular concentration of sulfite, reported to range from <20 nM (free sulfite) to 0.47-4.6 μM (free + bound sulfite) in serum and plasma.[59, 109] These values are much lower than the K_M for sulfite (260 ± 30 μM) that has been reported for the SQOR reaction.[54] Although higher sulfite levels in rat liver (9.2 μM) and heart (38 μM) were reported by the authors who proposed sulfite as a co-substrate for SQOR,[110] the lack of rigorous product identification raised questions about the validity of these values.[54] Since sulfite is inherently toxic[111-112] and is itself an oxidation product of sulfide, its use as a substrate for sulfide oxidation appears unlikely. Further, the buildup of toxic sulfite is averted by the activity of sulfite oxidase ($k_{cat}/K_{M\ (sulfite)}$ = ~2.4×10^6 $M^{-1}s^{-1}$).[58] However, under pathological conditions discussed above that lead to elevated sulfite, its use as an acceptor in the SQOR reaction might increase in significance.

In contrast to sulfite, GSH is highly abundant in cells (1-10 mM),[113-114] but is less efficient as an acceptor in the SQOR reaction ($k_{cat}/K_{M\ (GSH)}$ = 1.1×10^4 $M^{-1}s^{-1}$).[54] The $K_{M(GSH)}$ for the SQOR

reaction was initially determined to be 22 ± 3 mM,[53] and later revised to 8 ± 1 mM after accounting for a non-enzymatic reduction of CoQ_1 by GSH.[54] Incorporation of solubilized SQOR into nanodiscs slightly enhances the catalytic efficiencies of the reaction with either of the acceptors, with k_{cat}/K_M values of 2.5×10^6 M^{-1} s^{-1} and 1.6×10^4 M^{-1} s^{-1} for sulfite and GSH, respectively.[54] Kinetic simulations based on these values, and the intracellular concentrations of GSH and sulfite, predict that GSH is the dominant acceptor under physiological conditions.[53-54] The product, GSSH, is an efficient substrate for ETHE1 and is also the favored substrate for rhodanese, which converts GSSH to thiosulfate (Figure 2B). The pK_a of GSSH is 5.45 (versus 8.94 for GSH) and it exists almost exclusively as the persulfide anion (GSS^-) under physiological conditions.[115] This species is highly nucleophilic, which would prime it for facilitating cysteine persulfidation on proteins.

3.5. Structural basis for substrate promiscuity

The structural underpinnings of promiscuity that affords access to both small and bulky substrates[52-54, 93] became apparent from the structure of human SQOR. An early model of human SQOR[81] based on a bacterial enzyme structure presumed an active site comprising a cysteine disulfide on the *re* face of the FAD cofactor that was protected from solvent by capping loops that exist in some bacterial SQORs.[69-70] However, the crystal structure of human SQOR revealed that on the mitochondrial matrix side, a large electropositive cavity leads into the active site, and the orientation of the cysteine trisulfide causes ^{379}Cys to protrude into the cavity (Figure 8A).[72-73] This exposure to bulk solvent favors ^{379}Cys as the site of sulfide addition. The FAD cofactor is buried and shielded from solvent by a loop that spans residues ^{195}Pro to ^{203}Gly and includes ^{201}Cys, which is positioned proximal to the isoalloxazine ring of FAD. Based on substrate docking models, the cavity can accommodate the GSH tripeptide with its thiol moiety positioned to accept the sulfane sulfur on ^{379}Cys[72-73] (Figure 8B). Consequently, this cavity, which is large enough to accommodate GSH or CoA, also allows facile access to lower molecular weight acceptors including sulfite[53-54, 72] and methanethiol.[93] Presumably, substrate promiscuity is limited by the lower abundance of these acceptors relative to GSH and by the membrane environment of SQOR.[93]

4. Sulfide oxidation and its influence on metabolic pathways

4.1. Sulfide has bimodal effects on oxidative phosphorylation

A role for H_2S oxidation in energy production has been known for decades with SQOR contributing to membrane-bound electron transport in autotrophic and chemolithotrophic bacteria,[116-118] archaea,[119] and eukarya.[120] Sulfide-driven quinone reduction attributable to SQOR activity was first reported in membranes of the green sulfur bacterium *Chlorobium thiosulfatophilum* in which H_2S oxidation is coupled to the electron transport chain and reduction of $NADP^+$.[121] Similarly, coupling of sulfide oxidation to quinone reduction and energy production in *Rhodobacter sulfidophilus*[122] and the cyanobacterium *Oscillatoria limnetica*,[123] have been reported. The link between H_2S oxidation and oxidative phosphorylation was initially investigated

in eukaryotes that are adapted to high environmental sulfide exposure, such as the bivalve *Solemya reidi*,[124-125] the killifish *Fundulus parvipinnis*,[126] and the lugworm *Arenicola marina*.[127-128] Studies on *A. marina* SQOR revealed that sulfide oxidation leads to CoQ reduction and entry into the electron transfer chain at the level of Complex III.[129]

H_2S stimulates mitochondrial respiration at lower concentrations but inhibits it at higher concentrations, as seen in studies with isolated human mitochondria and in cell lines by monitoring oxygen consumption kinetics.[8, 82, 130] Cellular capacity for H_2S oxidation is dependent in part on SQOR levels, and its overexpression in Chinese hamster ovary cells decreases sensitivity to respiratory poisoning by H_2S.[130] Conversely, SQOR knockdown in HT-29 cells increases susceptibility to respiratory poisoning by H_2S.[8] SQOR and the downstream sulfide oxidation enzymes, ETHE1 and rhodanese, are expressed at higher levels in colorectal cancer tissue as well as in multiple human colon cancer cell lines, which are more resistant to H_2S versus non-malignant colon epithelial cells.[8] Increased expression of the sulfide oxidation pathway enzymes in cancer cells may thus counteract the anti-proliferative effects of H_2S exposure.[8] Inhibition of Complex IV by H_2S with consequent build-up of the $CoQH_2$ pool, could reverse electron flow through Complex II, leading to conversion of fumarate to succinate.[82] Succinate accumulation is observed in ischemia, and restoration of Complex II activity in the forward direction during reperfusion leads to rapid oxidation of succinate, with concomitant reduction of the CoQ pool, which drives reverse electron transfer and ROS production at Complex I, contributing to tissue injury.[131] It has not been clearly established whether complex IV inhibition induces H_2S oxidation via reversal of electron flow through Complex II and/or whether $CoQH_2$ can drive reversal of electron flow through SQOR itself, leading to ROS production. Other mitochondrial flavoenzymes that connect to the electron transport chain, including dihydroorotate dehydrogenase[132] and glycerol-3-phosphate dehydrogenase,[133] can oxidize $CoQH_2$, forming ROS.

4.2. Sulfide induces a reprogramming of mitochondrial bioenergetics

Sulfide oxidation by SQOR can exert a direct influence on bioenergetics via the mitochondrial CoQ pool, which represents a major redox nexus. Coupling of SQOR activity to the CoQ pool creates intersections between sulfide metabolism and: (i) Complex I, which oxidizes NADH, (ii) Complex II, which oxidizes succinate and $FADH_2$, (iii) dihydroorotate dehydrogenase, which is involved in *de novo* pyrimidine biosynthesis,[134] (iv) glycerol-3-phosphate dehydrogenase, which links to both carbohydrate and lipid metabolism,[135] and (v) the electron-transferring flavoprotein dehydrogenase, which is involved in fatty acid and branched chain amino acid metabolism.[136] Acute exposure to high H_2S levels in the colon, with a consequent decrease in the $CoQ/CoQH_2$ ratio could limit other activities that rely on an oxidized CoQ pool. Thus, in addition to respiratory inhibition, H_2S oxidation can also inhibit other oxidative metabolic pathways.

Thus, hyper-reduction of the CoQ pool, like mitochondrial dysfunction,[137] can lead to a decrease in the mitochondrial $NAD^+/NADH$ ratio, limiting electron acceptor and uridine availability. Indeed, treatment of malignant colon cell lines with H_2S restricts cell proliferation, which can be restored by exogenous pyruvate and uridine, demonstrating that acute exposure to

high H_2S leads to electron acceptor insufficiency.[8] These cells also become deficient in aspartate synthesis, which also requires NAD^+ for synthesis from carbon sources such as glucose or glutamine as demonstrated in cells with mitochondrial dysfunction.[138-139] The reductive stress in H_2S-treated cells is partially alleviated by metabolic rewiring of the citric acid cycle via reductive carboxylation of α-ketoglutarate to citrate. SQOR activity can therefore trigger metabolite signaling via alterations in mitochondrial redox homeostasis.[8]

4.3 Inherited Deficiency of SQOR

Inborn errors in SQOR metabolism have been identified recently in three children from two unrelated families and were associated with severe metabolic abnormalities resembling Leigh disease.[140] Disease onset varied between ~4 to 8 years of age, and the acute symptoms were triggered by fasting or infection. The symptoms included lactic acidosis, multi-organ failure, neurological disorders, and Leigh-like brain lesions. Two patients who were siblings were homozygous for the Glu213Lys mutation, affecting a residue that is remote from the active site, but predicted to disrupt hydrogen bonding with neighboring arginine residues. The third patient was homozygous for a single base pair deletion (c446delT) in the SQOR gene, predicted to lead to mRNA degradation or production of non-functional enzyme due to the resulting frameshift. The mutations led to greatly diminished SQOR levels in tissues expressing the Glu213Lys mutation while SQOR was not detected in fibroblasts carrying the deletion mutation. Complex IV activity but not its assembly was adversely affected by SQOR deficiency. Notably, the gastrointestinal defects and accumulation of acylcarnitines reported for ETHE1 deficiency[141] were not seen in SQOR deficiency,[140] although elevated H_2S was reported for both conditions.

4.4. The role of SQOR in proteostasis

Studies on *Caenorhabditis elegans* have implicated SQOR as a mediator of the unfolded protein response that was induced by exposure to H_2S,[142] which also led to enhanced thermotolerance and increased lifespan.[143-144] Significant effects on protein translation due to H_2S treatment are observed in *C. elegans* upon deletion of *sqrd-1* encoding a putative SQOR. These effects include reduced incorporation of ^{35}S-labeled methionine into proteins and an increase in free ribosomal subunits and translation factors.[142] Translational perturbations in the *sqrd-1* mutant *C. elegans* were traced to an increase in eIF2α phosphorylation upon H_2S exposure, leading to the induction of ER and mitochondrial stress responses.[142] Based on these results, SQOR was proposed to play a role in proteostasis.

In mammalian cells, accumulation of phosphorylated eIF2α and decreased protein synthesis were observed upon exposure to exogenous H_2S, or stimulation of CSE-dependent H_2S synthesis.[145] Phosphorylation of eIF2α was reversible and traced to the protein phosphatase PP1c, which was persulfidated upon H_2S treatment. H_2S-induced accumulation of eIF2α phosphorylation led to pre-conditioning, which partially protected cells from subsequent ER stress-induced cell death. While the role of SQOR was not investigated, protective persulfidation might play a role in

the H_2S-based modulation of the integrated stress response, shielding proteins from irreversible oxidative damage.

4.5. Interplay of sulfide oxidation and butyrate oxidation

H_2S concentrations in the colon are higher than in other tissues by several orders of magnitude,[42-43] due to microbial H_2S production.[44-45] Correspondingly, colonocytes are adapted to withstand acute exposure to high H_2S.[106] The primary fuel source for these cells is butyrate, a short-chain fatty acid produced by gut microbiota via fermentation of insoluble fiber remnants.[146-148] The first step in butyrate oxidation is catalyzed by butyryl-CoA dehydrogenase (ACADS), a flavoenzyme residing in the mitochondrial matrix. ACADS oxidizes butyryl-CoA to crotonyl-CoA, with the resulting electrons relayed to the electron transferring flavoprotein, ETF. ETF subsequently reduces ETF dehydrogenase in the inner mitochondrial membrane, where electrons enter the CoQ pool. As discussed above, because sulfide oxidation by SQOR also drives electrons into the CoQ pool, acute H_2S exposures can be challenging for energy production in colonocytes.

Sulfide inhibits butyrate oxidation in colonocytes, which mimics the conditions seen in ulcerative colitis and implicates sulfide as a factor in its pathology.[49-50] This inhibition is marked by increased butyryl-CoA levels and decreased crotonyl-CoA levels,[50] suggesting the involvement of ACADS. A mysteriously stable "green" ACADS was isolated decades ago from bovine, ovine, and porcine liver[149-152] and bacteria.[153] While the green color was later assigned to a CT complex between FAD and a tightly-bound coenzyme A persulfide (CoA-SSH),[105] the intracellular source of CoA-SSH remained unknown. We recently demonstrated that the substrate promiscuity of SQOR extends to CoA, supporting the synthesis of CoA-SSH, which in turn inhibits ACADS forming a CT complex.[73] We proposed that SQOR-catalyzed CoA-SSH production and subsequent inhibition of ACADS, thereby prioritizes the CoQ pool for sulfide over butyrate oxidation (Figure 9).

Summary and Outlook

The high efficiency of sulfide oxidation catalyzed by SQOR serves as a protective shield against respiratory poisoning and triggers transient reprogramming of mitochondrial metabolism via inhibition of Complex IV. Inherited deficiency of SQOR presents as a newly described cause of Leigh disease with decreased Complex IV activity. On the other hand, H_2S oxidation leads to the formation of highly reactive persulfides, which could be important for protein persulfidation, a modification that is increased in cells following H_2S exposure. It is presently not known whether the primary role of SQOR is to activate H_2S by forming persulfides while simultaneously preventing its toxic accumulation or signaling via perturbations in electron transport chain, or both.

Structural and biochemical characterization of SQOR continues to surprise, revealing a unique catalytic cysteine trisulfide, and a persulfide-based CT complex with FAD. The promiscuity of SQOR can be traced to the large electropositive entrance to the active site that accommodates a range of substrates and has the potential to generate a variety of low molecular weight persulfides. The production of CoA-SSH, long known as a tight binding inhibitor of ACADS, has recently

been traced to the relaxed substrate specificity of SQOR and could prioritize sulfide over butyrate oxidation during acute colonic exposure to H_2S. It is not known whether other persulfides are produced via SQOR in a tissue-specific manner and in response to intra- or extra-cellular triggers. A deeper understanding of the structure and mechanism of SQOR will facilitate its therapeutic targeting in H_2S-related pathologies.

Acknowledgements
This work was supported by the National Institutes of Health (GM130183 to R.B.).

Conflict of Interest
The authors declare no conflict of interest.

References

[1] W. P. Yant, *Am. J. Public Health* **1930,** *20*, 598-608
[2] C. L. Evans, *Q. J. Exp. Physiol. Cogn. Med. Sci.* **1967,** *52*, 231-248
[3] F. Bouillaud, F. Blachier, *Antioxid. Redox Signal.* **2011,** *15*, 379-391
[4] R. O. Beauchamp, Jr., J. S. Bus, J. A. Popp, C. J. Boreiko, D. A. Andjelkovich, *Crit. Rev. Toxicol.* **1984,** *13*, 25-97
[5] K. Abe, H. Kimura, *J. Neurosci.* **1996,** *16*, 1066–1071
[6] H. Kimura, *Antioxid. Redox Signal.* **2010,** *12*, 1111–1123
[7] V. Vitvitsky, O. Kabil, R. Banerjee, *Antioxid. Redox Signal.* **2012,** *17*, 22–31
[8] M. Libiad, V. Vitvitsky, T. Bostelaar, D. W. Bak, H. J. Lee, N. Sakamoto, E. Fearon, C. A. Lyssiotis, E. Weerapana, R. Banerjee, *J. Biol. Chem.* **2019,** *294*, 12077-12090
[9] E. A. Peter, X. Shen, S. H. Shah, S. Pardue, J. D. Glawe, W. W. Zhang, P. Reddy, N. I. Akkus, J. Varma, C. G. Kevil, *J. Am. Heart Assoc.* **2013,** *2*, e000387
[10] C. Szabo, C. Coletta, C. Chao, K. Modis, B. Szczesny, A. Papapetropoulos, M. R. Hellmich, *Proc. Natl. Acad. Sci. U. S. A.* **2013,** *110*, 12474–12479
[11] E. A. Ostrakhovitch, S. Akakura, R. Sanokawa-Akakura, S. Goodwin, S. Tabibzadeh, *Exp. Cell Res.* **2015,** *330*, 135–150
[12] C. Coletta, C. Szabo, *Curr. Vasc. Pharmacol.* **2013,** *11*, 208–221
[13] D. Chen, H. Pan, C. Li, X. Lan, B. Liu, G. Yang, *J. Huazhong Univ. Sci. Technol. (Health Sci.)* **2011,** *31*, 632–636
[14] S. F. Ang, S. M. Moochhala, P. A. MacAry, M. Bhatia, *PLoS One* **2011,** *6*, e24535
[15] L. Sun, S. Sun, Y. Li, W. Pan, Y. Xie, S. Wang, Z. Zhang, *Chin. Med. J.* **2014,** *127*, 893–899
[16] S. Mani, H. Li, A. Untereiner, L. Wu, G. Yang, R. C. Austin, J. G. Dickhout, S. Lhotak, Q. H. Meng, R. Wang, *Circulation* **2013,** *127*, 2523–2534
[17] L. Fang, H. Li, C. Tang, B. Geng, Y. Qi, X. Liu, *Can. J. Physiol. Pharmacol.* **2009,** *87*, 531–538
[18] G. Tan, S. Pan, J. Li, X. Dong, K. Kang, M. Zhao, X. Jiang, J. R. Kanwar, H. Qiao, H. Jiang, X. Sun, *PLoS One* **2011,** *6*, e25943
[19] E. Blackstone, M. Morrison, M. B. Roth, *Science* **2005,** *308*, 518
[20] C. Szabo, *Nat. Rev. Drug. Discov.* **2007,** *6*, 917–935
[21] J. L. Wallace, R. W. Blackler, M. V. Chan, G. J. Da Silva, W. Elsheikh, K. L. Flannigan, I. Gamaniek, A. Manko, L. Wang, J. P. Motta, A. G. Buret, *Antioxid. Redox Signal.* **2015,** *22*, 398–410
[22] M. D. Maines, *Annu. Rev. Pharmacol. Toxicol.* **1997,** *37*, 517-554
[23] L. J. Ignarro, *Biosci. Rep.* **1999,** *19*, 51–71
[24] A. K. Mustafa, M. M. Gadalla, S. H. Snyder, *Sci. Signal.* **2009,** *2*, re2
[25] A. K. Mustafa, M. M. Gadalla, N. Sen, S. Kim, W. Mu, S. K. Gazi, R. K. Barrow, G. Yang, R. Wang, S. H. Snyder, *Sci. Signal.* **2009,** *2*, ra72
[26] K. Y. Chen, J. C. Morris, *Environ. Sci. Technol.* **1972,** *6*, 529-537
[27] T. V. Mishanina, M. Libiad, R. Banerjee, *Nat. Chem. Biol.* **2015,** *11*, 457–464
[28] M. Libiad, N. Motl, D. L. Akey, N. Sakamoto, E. R. Fearon, J. L. Smith, R. Banerjee, *J. Biol. Chem.* **2018,** *293*, 2675–2686
[29] X. H. Gao, D. Krokowski, B. J. Guan, I. Bederman, M. Majumder, M. Parisien, L. Diatchenko, O. Kabil, B. Willard, R. Banerjee, B. Wang, G. Bebek, C. R. Evans, P. L. Fox, S. L. Gerson, C. L. Hoppel, M. Liu, P. Arvan, M. Hatzoglou, *eLife* **2015,** *4*, e10067

[30] E. Cuevasanta, M. N. Moller, B. Alvarez, *Arch. Biochem. Biophys.* **2017,** *617*, 9-25
[31] M. R. Filipovic, J. Zivanovic, B. Alvarez, R. Banerjee, *Chem. Rev.* **2018,** *118*, 1253–1337
[32] P. W. Beatty, D. J. Reed, *Arch. Biochem. Biophys.* **1980,** *204*, 80-87
[33] E. Mosharov, M. R. Cranford, R. Banerjee, *Biochemistry* **2000,** *39*, 13005-13011
[34] S. Singh, R. Banerjee, *Biochim. Biophys. Acta* **2011,** *1814*, 1518-1527
[35] T. Chiku, D. Padovani, W. Zhu, S. Singh, V. Vitvitsky, R. Banerjee, *J. Biol. Chem.* **2009,** *284*, 11601–11612
[36] S. Singh, D. Padovani, R. A. Leslie, T. Chiku, R. Banerjee, *J. Biol. Chem.* **2009,** *284*, 22457–22466
[37] O. Kabil, V. Vitvitsky, P. Xie, R. Banerjee, *Antioxid. Redox Signal.* **2011,** *15*, 363-372
[38] P. K. Yadav, K. Yamada, T. Chiku, M. Koutmos, R. Banerjee, *J. Biol. Chem.* **2013,** *288*, 20002–20013
[39] P. K. Yadav, V. Vitvitsky, S. Carballal, J. Seravalli, R. Banerjee, *J. Biol. Chem.* **2020,** *295*, 6299-6311
[40] J. Furne, A. Saeed, M. D. Levitt, *Am. J. Physiol. Regul. Integr. Comp. Physiol.* **2008,** *295*, R1479–1485
[41] M. D. Levitt, M. S. Abdel-Rehim, J. Furne, *Antioxid. Redox Signal.* **2011,** *15*, 373-378
[42] G. T. Macfarlane, G. R. Gibson, J. H. Cummings, *J. Appl. Bacteriol.* **1992,** *72*, 57–64
[43] B. Deplancke, K. Finster, W. V. Graham, C. T. Collier, J. E. Thurmond, H. R. Gaskins, *Exp. Biol. Med. (Maywood)* **2003,** *228*, 424-433
[44] P. J. Turnbaugh, J. I. Gordon, *J. Physiol.* **2009,** *587*, 4153-4158
[45] D. R. Linden, *Antioxid. Redox Signal.* **2014,** *20*, 818-830
[46] J. C. Mathai, A. Missner, P. Kugler, S. M. Saparov, M. L. Zeidel, J. K. Lee, P. Pohl, *Proc. Natl. Acad. Sci. U. S. A.* **2009,** *106*, 16633-16638
[47] C. Atuma, V. Strugala, A. Allen, L. Holm, *Am. J. Physiol. Gastrointest. Liver Physiol.* **2001,** *280*, G922-929
[48] M. E. Johansson, K. A. Thomsson, G. C. Hansson, *J. Proteome Res.* **2009,** *8*, 3549-3557
[49] W. E. Roediger, A. Duncan, O. Kapaniris, S. Millard, *Clin. Sci.* **1993,** *85*, 623-627
[50] W. Babidge, S. Millard, W. Roediger, *Mol. Cell. Biochem.* **1998,** *181*, 117-124
[51] T. M. Hildebrandt, M. K. Grieshaber, *FEBS J.* **2008,** *275*, 3352–3361
[52] M. R. Jackson, S. L. Melideo, M. S. Jorns, *Biochemistry* **2012,** *51*, 6804–6815
[53] M. Libiad, P. K. Yadav, V. Vitvitsky, M. Martinov, R. Banerjee, *J. Biol. Chem.* **2014,** *289*, 30901–30910
[54] A. P. Landry, D. P. Ballou, R. Banerjee, *J. Biol. Chem.* **2017,** *292*, 11641–11649
[55] V. Tiranti, C. Viscomi, T. Hildebrandt, I. Di Meo, R. Mineri, C. Tiveron, M. D. Levitt, A. Prelle, G. Fagiolari, M. Rimoldi, M. Zeviani, *Nat. Med.* **2009,** *15*, 200–205
[56] O. Kabil, R. Banerjee, *J. Biol. Chem.* **2012,** *287*, 44561–44567
[57] M. Libiad, A. Sriraman, R. Banerjee, *J. Biol. Chem.* **2015,** *290*, 23579-23588
[58] K. Johnson-Winters, A. R. Nordstrom, S. Emesh, A. V. Astashkin, A. Rajapakshe, R. E. Berry, G. Tollin, J. H. Enemark, *Biochemistry* **2010,** *49*, 1290-1296
[59] T. Togawa, M. Ogawa, M. Nawata, Y. Ogasawara, K. Kawanabe, S. Tanabe, *Chem. Pharm. Bull.* **1992,** *40*, 3000–3004
[60] D. E. Cole, J. Evrovski, *J. Chromatogr. A* **1997,** *789*, 221-232
[61] D. E. Cole, J. Evrovski, R. Pirone, *J. Chromatogr. B Biomed. Appl.* **1995,** *672*, 149-154
[62] D. E. Cole, J. Evrovski, *Clin. Chem.* **1996,** *42*, 654-655

[63] S. Kage, K. Takekawa, K. Kurosaki, T. Imamura, K. Kudo, *Int. J. Legal Med.* **1997,** *110*, 220-222
[64] M. Durand, P. Weinstein, *Forensic Toxicol.* **2007,** *25*, 92-95
[65] A. Argyrou, J. S. Blanchard, *Prog. Nucleic Acid Res. Mol. Biol.* **2004,** *78*, 89–142
[66] S. M. Miller, *Handbook of Flavoproteins: Volume 2 Complex Flavoproteins, Dehydrogenases and Physical Methods (de Gruyter) 1st ed, Vol. 2*, **2013**, 165-202.
[67] A. Claiborne, T. C. Mallett, J. I. Yeh, J. Luba, D. Parsonage, *Adv. Protein Chem.* **2001,** *58*, 215-276
[68] J. R. Wallen, T. C. Mallett, W. Boles, D. Parsonage, C. M. Furdui, P. A. Karplus, A. Claiborne, *Biochemistry* **2009,** *48*, 9650-9667
[69] M. Marcia, U. Ermler, G. Peng, H. Michel, *Proc. Natl. Acad. Sci. U. S. A.* **2009,** *106*, 9625–9630
[70] J. A. Brito, F. L. Sousa, M. Stelter, T. M. Bandeiras, C. Vonrhein, M. Teixeira, M. M. Pereira, M. Archer, *Biochemistry* **2009,** *48*, 5613–5622
[71] M. M. Cherney, Y. Zhang, M. Solomonson, J. H. Weiner, M. N. James, *J. Mol. Biol.* **2010,** *398*, 292–305
[72] M. R. Jackson, P. J. Loll, M. S. Jorns, *Structure* **2019,** *27*, 794-805 e794
[73] A. P. Landry, S. Moon, H. Kim, P. K. Yadav, A. Guha, U. S. Cho, R. Banerjee, *Cell Chem. Biol.* **2019,** *26*, 1515-1525 e1514
[74] U. Theissen, M. Hoffmeister, M. Grieshaber, W. Martin, *Mol. Biol. Evol.* **2003,** *20*, 1564-1574
[75] V. H. Pham, J. J. Yong, S. J. Park, D. N. Yoon, W. H. Chung, S. K. Rhee, *Microbiology* **2008,** *154*, 3112-3121
[76] M. Marcia, U. Ermler, G. Peng, H. Michel, *Proteins* **2010,** *78*, 1073-1083
[77] F. M. Sousa, J. G. Pereira, B. C. Marreiros, M. M. Pereira, *Biochim. Biophys. Acta, Bioenerg.* **2018,** *1859*, 742-753
[78] Z. W. Chen, M. Koh, G. Van Driessche, J. J. Van Beeumen, R. G. Bartsch, T. E. Meyer, M. A. Cusanovich, F. S. Mathews, *Science* **1994,** *266*, 430-432
[79] M. Reinartz, J. Tschape, T. Bruser, H. G. Truper, C. Dahl, *Arch. Microbiol.* **1998,** *170*, 59-68
[80] N. U. Frigaard, C. Dahl, *Adv. Microb. Physiol.* **2009,** *54*, 103-200
[81] T. V. Mishanina, P. K. Yadav, D. P. Ballou, R. Banerjee, *J. Biol. Chem.* **2015,** *290*, 25072–25080
[82] M. Goubern, M. Andriamihaja, T. Nubel, F. Blachier, F. Bouillaud, *FASEB J.* **2007,** *21*, 1699–1706
[83] M. M. Cherney, Y. Zhang, M. N. James, J. H. Weiner, *J. Struct. Biol.* **2012,** *178*, 319-328
[84] A. M. Jespersen, T. Christensen, N. K. Klausen, F. Nielsen, H. H. Sorensen, *Eur. J. Biochem.* **1994,** *219*, 365-373
[85] M. K. Thomsen, B. S. Hansen, P. Nilsson, J. Nowak, P. B. Johansen, P. D. Thomsen, J. Christiansen, *Pharmacol. Toxicol.* **1994,** *74*, 351-358
[86] C. Andersson, P. O. Edlund, P. Gellerfors, Y. Hansson, E. Holmberg, C. Hult, S. Johansson, J. Kordel, R. Lundin, I. B. Mendel-Hartvig, B. Noren, T. Wehler, G. Widmalm, J. Ohman, *Int. J. Pept. Protein Res.* **1996,** *47*, 311-321
[87] E. Canova-Davis, I. P. Baldonado, R. C. Chloupek, V. T. Ling, R. Gehant, K. Olson, B. L. Gillece-Castro, *Anal. Chem.* **1996,** *68*, 4044-4051

[88] A. A. Santos, S. S. Venceslau, F. Grein, W. D. Leavitt, C. Dahl, D. T. Johnston, I. A. Pereira, *Science* **2015,** *350*, 1541-1545
[89] A. P. Landry, S. Moon, J. Bonanata, U. S. Cho, E. L. Coitino, R. Banerjee, *J. Am. Chem. Soc.* **2020,** *142*, 14295-14306
[90] T. Ida, T. Sawa, H. Ihara, Y. Tsuchiya, Y. Watanabe, Y. Kumagai, M. Suematsu, H. Motohashi, S. Fujii, T. Matsunaga, M. Yamamoto, K. Ono, N. O. Devarie-Baez, M. Xian, J. M. Fukuto, T. Akaike, *Proc. Natl. Acad. Sci. U. S. A.* **2014,** *111*, 7606-7611
[91] P. K. Yadav, M. Martinov, V. Vitvitsky, J. Seravalli, R. Wedmann, M. R. Filipovic, R. Banerjee, *J. Am. Chem. Soc.* **2016,** *138*, 289-299
[92] E. Cuevasanta, M. Lange, J. Bonanata, E. L. Coitino, G. Ferrer-Sueta, M. R. Filipovic, B. Alvarez, *J. Biol. Chem.* **2015,** *290*, 26866–26880
[93] A. P. Landry, D. P. Ballou, R. Banerjee, *ACS Chem. Biol.* **2018,** *13*, 1651-1658
[94] V. E. Shih, I. F. Abroms, J. L. Johnson, M. Carney, R. Mandell, R. M. Robb, J. P. Cloherty, K. V. Rajagopalan, *N. Engl. J. Med.* **1977,** *297*, 1022–1028
[95] A. S. Vincent, B. G. Lim, J. Tan, M. Whiteman, N. S. Cheung, B. Halliwell, K. P. Wong, *Kidney Int.* **2004,** *65*, 393–402
[96] M. Grings, A. P. Moura, B. Parmeggiani, G. F. Marcowich, A. U. Amaral, A. T. de Souza Wyse, M. Wajner, G. Leipnitz, *Gene* **2013,** *531*, 191–198
[97] A. Iatropoulos, V. Panis, E. Mela, T. Stefaniotis, P. N. Madianos, W. Papaioannou, *J. Clin. Periodontol.* **2016,** *43*, 359–365
[98] A. Pol, G. H. Renkema, A. Tangerman, E. G. Winkel, U. F. Engelke, A. P. M. de Brouwer, K. C. Lloyd, R. S. Araiza, L. van den Heuvel, H. Omran, H. Olbrich, M. Oude Elberink, C. Gilissen, R. J. Rodenburg, J. O. Sass, K. O. Schwab, H. Schafer, H. Venselaar, J. S. Sequeira, H. J. M. Op den Camp, R. A. Wevers, *Nat. Genet.* **2018,** *50*, 120–129
[99] V. Massey, G. Palmer, *J. Biol. Chem.* **1962,** *237*, 2347-2358
[100] V. Massey, C. H. Williams, Jr., *J. Biol. Chem.* **1965,** *240*, 4470-4480
[101] A. S. Abramovitz, V. Massey, *J. Biol. Chem.* **1976,** *251*, 5327-5336
[102] R. G. Matthews, C. H. Williams, Jr., *J. Biol. Chem.* **1976,** *251*, 3956-3964
[103] L. D. Arscott, S. Gromer, R. H. Schirmer, K. Becker, C. H. Williams, Jr., *Proc. Natl. Acad. Sci. U. S. A.* **1997,** *94*, 3621-3626
[104] T. E. Meyer, R. G. Bartsch, M. A. Cusanovich, *Biochemistry* **1991,** *30*, 8840-8845
[105] G. Williamson, P. C. Engel, J. P. Mizzer, C. Thorpe, V. Massey, *J. Biol. Chem.* **1982,** *257*, 4314–4320
[106] M. D. Levitt, J. Furne, J. Springfield, F. Suarez, E. DeMaster, *J. Clin. Invest.* **1999,** *104*, 1107–1114
[107] T. W. Szczepkowski, B. Skarzynski, M. Weber, *Nature* **1961,** *189*, 1007-1008
[108] A. Koj, J. Frendo, Z. Janik, *Biochem. J.* **1967,** *103*, 791–795
[109] A. J. Ji, S. R. Savon, D. W. Jacobsen, *Clin. Chem.* **1995,** *41*, 897–903
[110] K. D. Augustyn, M. R. Jackson, M. S. Jorns, *Biochemistry* **2017,** *56*, 986–996
[111] A. F. Gunnison, *Food Cosmet. Toxicol.* **1981,** *19*, 667-682
[112] A. Stammati, C. Zanetti, L. Pizzoferrato, E. Quattrucci, G. B. Tranquilli, *Food Addit. Contam.* **1992,** *9*, 551-560
[113] N. S. Kosower, E. M. Kosower, *Int. Rev. Cytol.* **1978,** *54*, 109–160
[114] A. Meister, *J. Biol. Chem.* **1988,** *263*, 17205–17208
[115] D. Benchoam, J. A. Semelak, E. Cuevasanta, M. Mastrogiovanni, J. S. Grassano, G. Ferrer-Sueta, A. Zeida, M. Trujillo, M. N. Möller, D. A. Estrin, *J. Biol. Chem.* **2020**, jbc-RA120

[116] D. C. Brune, *Anoxygenic Photosynthetic Bacteria (Springer, Dordrecht)* **1995**, 847-870.
[117] C. G. Friedrich, *Adv. Microb. Physiol.* **1998,** *39*, 235-289
[118] D. P. Kelly, J. K. Shergill, W. P. Lu, A. P. Wood, *Antonie Van Leeuwenhoek* **1997,** *71*, 95-107
[119] K. O. Stetter, *FEMS Microbiol. Rev.* **1996,** *18*, 149-158
[120] M. K. Grieshaber, S. Volkel, *Annu. Rev. Physiol.* **1998,** *60*, 33-53
[121] D. B. Knaff, B. B. Buchanan, *Biochim. Biophys. Acta* **1975,** *376*, 549-560
[122] D. C. Brune, H. G. Trüper, *Arch. Microbiol.* **1986,** *145*, 295-301
[123] B. Arieli, E. Padan, Y. Shahak, *J. Biol. Chem.* **1991,** *266*, 104–111
[124] J. O'Brien, R. D. Vetter, *J. Exp. Biol.* **1990,** *149*, 133-148
[125] M. A. Powell, G. N. Somero, *Science* **1986,** *233*, 563-566
[126] T. Bagarinao, R. D. Vetter, *J. Comp. Physiol., B* **1990,** *160*, 519-527
[127] S. Völkel, M. K. Grieshaber, *Mar. Biol.* **1994,** *118*, 137-147
[128] S. Völkel, M. K. Grieshaber, *Physiologist* **1994,** *37*, A88
[129] S. Volkel, M. K. Grieshaber, *Eur. J. Biochem.* **1996,** *235*, 231-237
[130] E. Lagoutte, S. Mimoun, M. Andriamihaja, C. Chaumontet, F. Blachier, F. Bouillaud, *Biochim. Biophys. Acta* **2010,** *1797*, 1500–1511
[131] E. T. Chouchani, V. R. Pell, E. Gaude, D. Aksentijevic, S. Y. Sundier, E. L. Robb, A. Logan, S. M. Nadtochiy, E. N. J. Ord, A. C. Smith, F. Eyassu, R. Shirley, C. H. Hu, A. J. Dare, A. M. James, S. Rogatti, R. C. Hartley, S. Eaton, A. S. H. Costa, P. S. Brookes, S. M. Davidson, M. R. Duchen, K. Saeb-Parsy, M. J. Shattock, A. J. Robinson, L. M. Work, C. Frezza, T. Krieg, M. P. Murphy, *Nature* **2014,** *515*, 431-435
[132] H. J. Forman, J. Kennedy, *Arch. Biochem. Biophys.* **1976,** *173*, 219-224
[133] L. Tretter, K. Takacs, V. Hegedus, V. Adam-Vizi, *J. Neurochem.* **2007,** *100*, 650-663
[134] D. R. Evans, H. I. Guy, *J. Biol. Chem.* **2004,** *279*, 33035-33038
[135] J. W. Harding, Jr., E. A. Pyeritz, E. S. Copeland, H. B. White, 3rd, *Biochem. J.* **1975,** *146*, 223-229
[136] N. J. Watmough, F. E. Frerman, *Biochim. Biophys. Acta* **2010,** *1797*, 1910-1916
[137] M. P. King, G. Attardi, *Science* **1989,** *246*, 500-503
[138] K. Birsoy, T. Wang, W. W. Chen, E. Freinkman, M. Abu-Remaileh, D. M. Sabatini, *Cell* **2015,** *162*, 540-551
[139] L. B. Sullivan, D. Y. Gui, A. M. Hosios, L. N. Bush, E. Freinkman, M. G. Vander Heiden, *Cell* **2015,** *162*, 552-563
[140] M. W. Friederich, A. F. Elias, A. Kuster, L. Laugwitz, A. A. Larson, A. P. Landry, L. Ellwood-Digel, D. M. Mirsky, D. Dimmock, J. Haven, *J. Inherit. Metab. Dis.* **2020,** *43*, 1024-1036
[141] V. Tiranti, P. D'Adamo, E. Briem, G. Ferrari, R. Mineri, E. Lamantea, H. Mandel, P. Balestri, M. T. Garcia-Silva, B. Vollmer, P. Rinaldo, S. H. Hahn, J. Leonard, S. Rahman, C. Dionisi-Vici, B. Garavaglia, P. Gasparini, M. Zeviani, *Am. J. Hum. Genet.* **2004,** *74*, 239-252
[142] J. W. Horsman, D. L. Miller, *J. Biol. Chem.* **2016,** *291*, 5320–5325
[143] D. L. Miller, M. B. Roth, *Proc. Natl. Acad. Sci. U. S. A.* **2007,** *104*, 20618-20622
[144] D. L. Miller, M. W. Budde, M. B. Roth, *PLoS One* **2011,** *6*, e25476
[145] V. Yadav, X. H. Gao, B. Willard, M. Hatzoglou, R. Banerjee, O. Kabil, *J. Biol. Chem.* **2017,** *292*, 13143-13153
[146] W. E. Roediger, *Gut* **1980,** *21*, 793-798

[147] H. M. Hamer, D. Jonkers, K. Venema, S. Vanhoutvin, F. J. Troost, R. J. Brummer, *Aliment. Pharmacol. Ther.* **2008,** *27,* 104-119
[148] G. den Besten, K. van Eunen, A. K. Groen, K. Venema, D. J. Reijngoud, B. M. Bakker, *J. Lipid Res.* **2013,** *54,* 2325-2340
[149] D. E. Green, S. Mii, H. R. Mahler, R. M. Bock, *J. Biol. Chem.* **1954,** *206,* 1-12
[150] H. R. Mahler, *J. Biol. Chem.* **1954,** *206,* 13-26
[151] E. P. Steyn-Parve, H. Beinert, *J. Biol. Chem.* **1958,** *233,* 853-861
[152] L. Shaw, P. C. Engel, *Biochem. J.* **1984,** *218,* 511-520
[153] P. C. Engel, V. Massey, *Biochem. J.* **1971,** *125,* 879-887

Figures

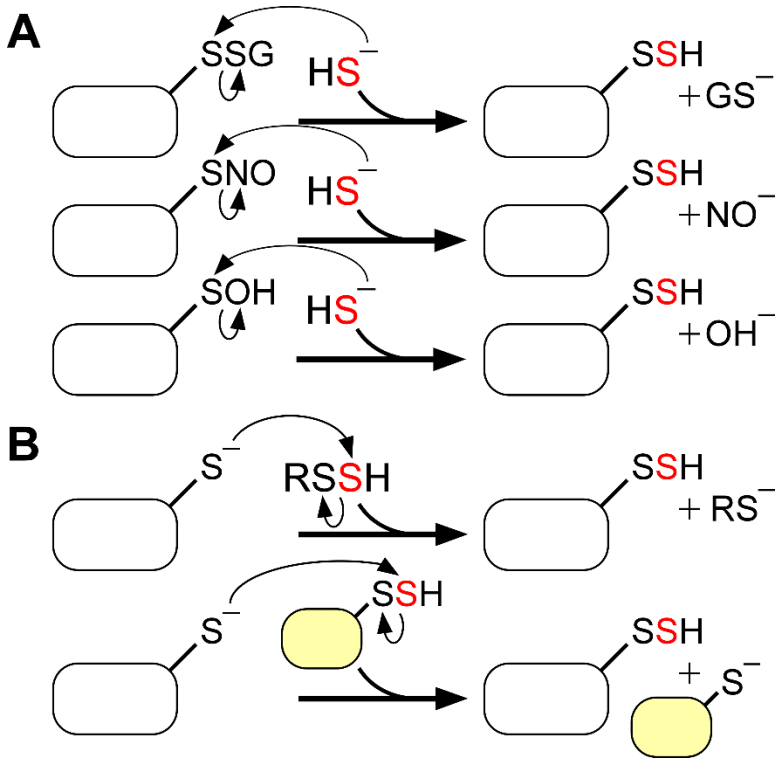

Figure 1. Mechanisms of protein persulfidation. A, Persulfidation of oxidized cysteines on proteins. **B**, Persulfidation of reduced cysteines on proteins via reaction with a low molecular weight persulfide (RSSH) or a sulfurtransferase.

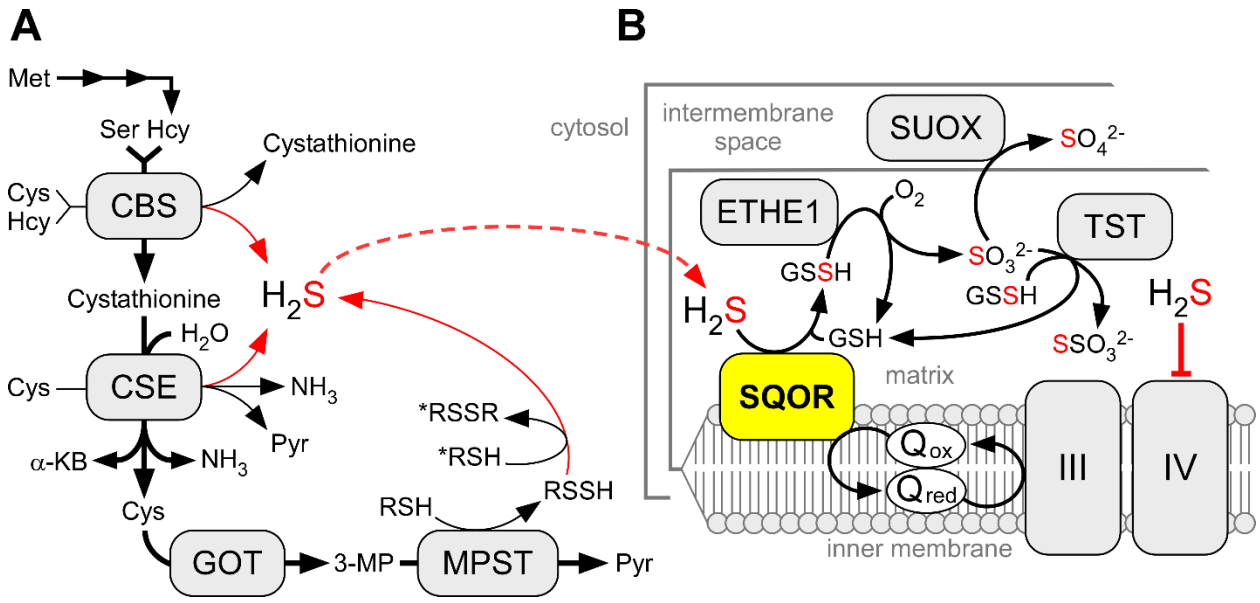

Figure 2. H_2S biosynthesis and oxidation pathways. A, The canonical reactions catalyzed by CBS and CSE and MPST are depicted by bold black arrows while the H_2S-synthesizing reactions are shown by thin black and red arrows. α-KB and Pyr denote α-ketobutyrate and pyruvate, respectively. GOT and 3-MP denote cysteine aminotransferase and its product, 3-mercaptopyruvate, respectively. To note, MPST has both cytoplasmic and mitochondrial isoforms. **B**, The mitochondrial sulfide oxidation pathway. TST, SUOX, III and IV denote rhodanese, sulfite oxidase, and respiratory complexes III and IV, respectively.

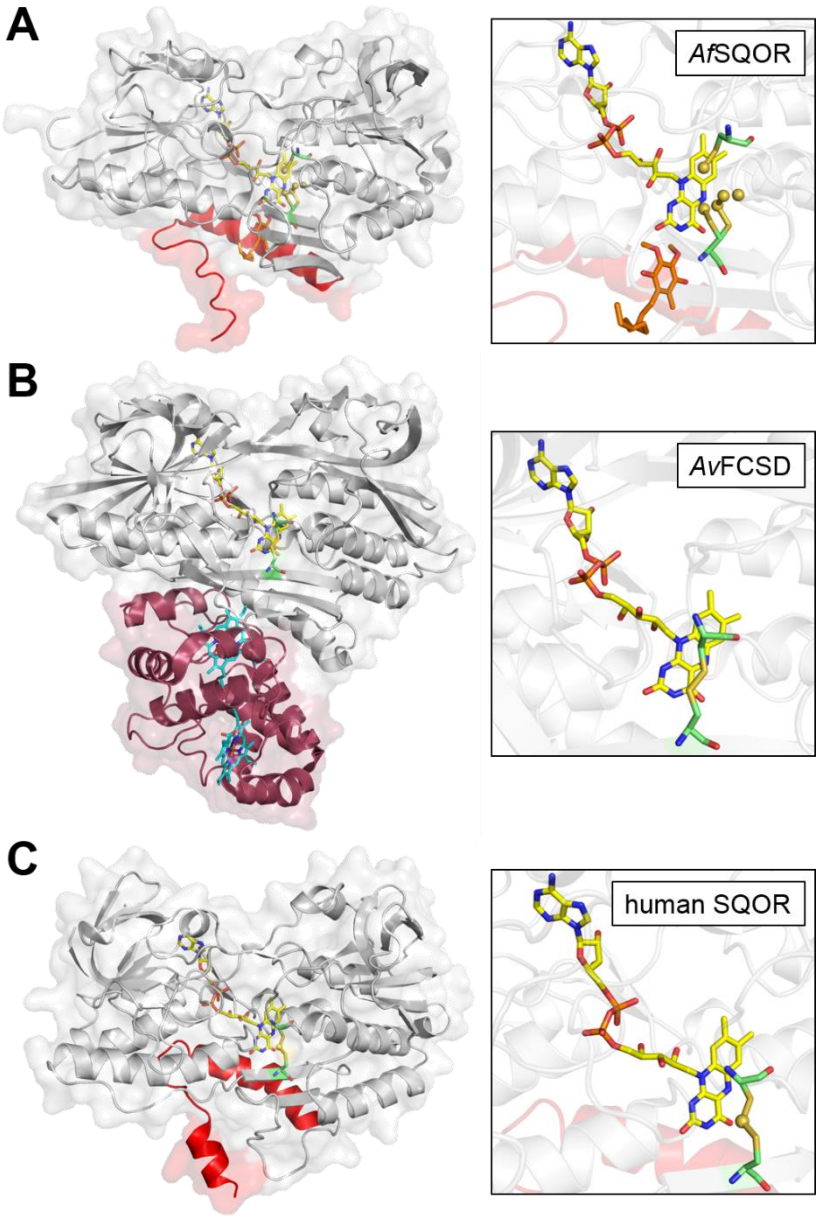

Figure 3. Structures of bacterial SQOR, FCSD, and human SQOR. Cartoon and transparent surface overlay representations of **A**, *Acidithiobacillus ferrooxidans* SQOR (*Af*SQOR, PDB ID: 3T31); **B**, *Allochromatium vinosum* FCSD (*Av*FCSD, PDB ID: 1FCD); and **C**, human SQOR (PDB ID: 6OI5). The amphipathic helices of membrane-anchored *Af*SQOR and human SQOR are depicted in red, and the diheme cytochrome subunit of cytosolic *Av*FCSD is depicted in burgundy. Yellow sticks represent the FAD cofactor in each structure. The CoQ analog decylubiquinone in *Af*SQOR is shown in orange stick display and the dual heme cofactors in the cytochrome subunit of *Av*FCSD in cyan. An enlarged view of the active sites is shown in each panel on the right, with the redox active cysteines displayed in green sticks. Sulfane sulfur atoms in *Af*SQOR and bridging the active site cysteines in human SQOR, are shown as yellow spheres.

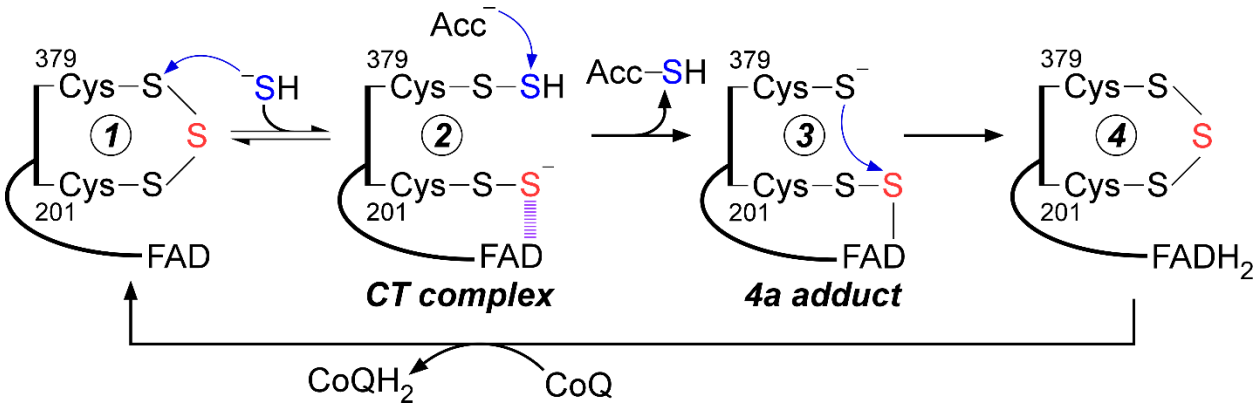

Figure 4. Proposed catalytic mechanism for human SQOR. The bridging sulfur within the active site cysteine trisulfide is shown in red. The sulfur that undergoes oxidation and transfer to a thiophilic acceptor (Acc) is shown in blue.

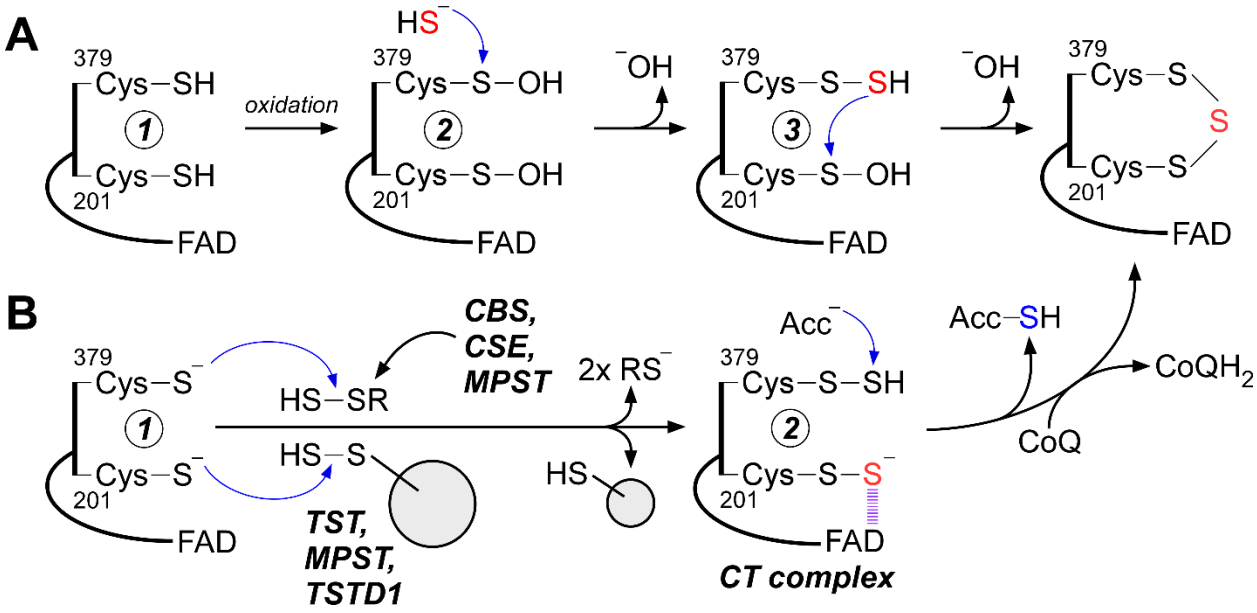

Figure 5. Possible mechanisms for *in vivo* building of the SQOR cysteine trisulfide. A, Oxidation of active site cysteines in newly synthesized SQOR (e.g., formation of cysteine sulfenic acid) (*2*) can promote cysteine persulfide formation (*3*) via nucleophilic attack of sulfide. Attack on the sulfenic acid by the persulfide generates the trisulfide. **B**, Persulfidation of SQOR at each cysteine by small molecule persulfides generated by the H_2S synthesizing enzymes (CBS: cystathionine β-synthase; CSE: cystathionine γ-lyase; MPST: 3-mercaptopyruvate sulfurtransferase), or by an enzyme-catalyzed sulfur transfer via a sulfurtransferase (TST: rhodanese; MPST, or TSTD1), generates the CT complex (*2*). The latter leads to cysteine trisulfide formation following electron transfer to FAD and subsequent oxidation by CoQ.

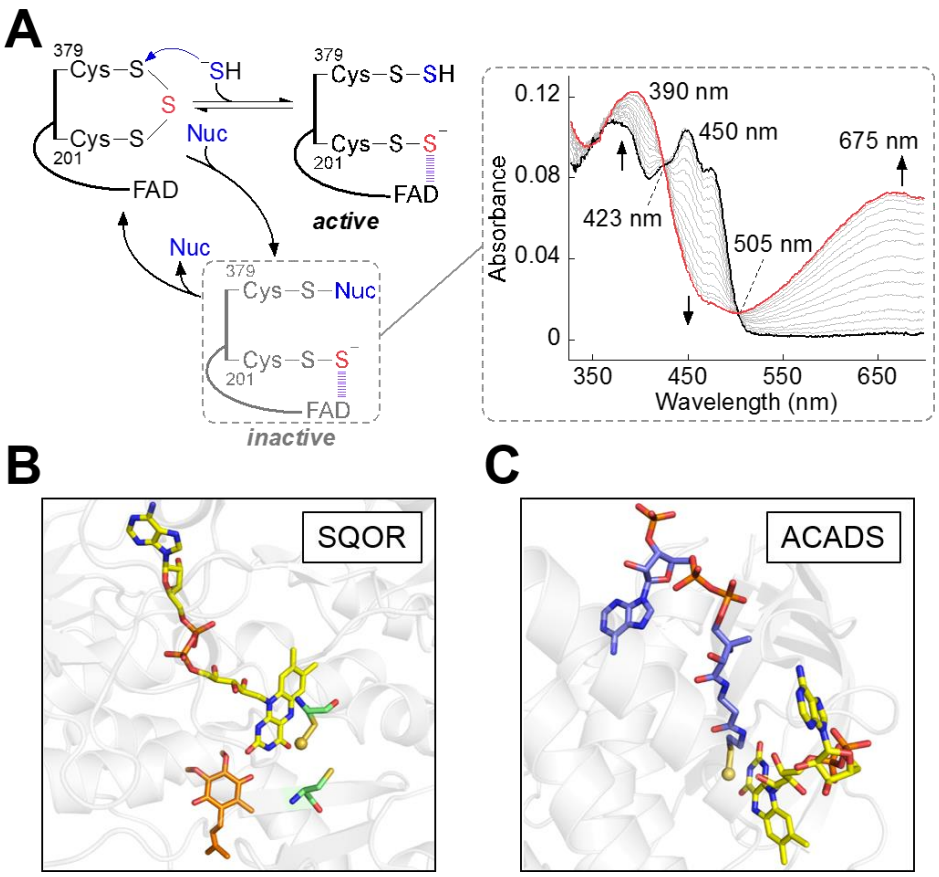

Figure 6. Promiscuous nucleophilic addition and active site persulfide formation. A, Alternative to sulfide, nucleophiles (Nuc) including GSH, sulfite, and methanethiol are capable of adding into the cysteine trisulfide to form a slowly decaying dead-end complex. The right panel (adapted from Ref. 93 Supplemental Figure 2) shows SQOR embedded in nanodiscs (20 μM, black trace) rapidly mixed with sulfite (500 μM) and monitored over a period of 14 s for the formation of an alternative CT complex (red trace), with an absorbance maximum at 675 nm. **B**, Active site of human SQOR co-crystallized with CoQ (orange sticks) and soaked with sulfite (PDB: 6OIC), which contained a stable ^{201}Cys persulfide-to-FAD CT complex *in crystallo*. C, Active site of ACADS crystallized with bound CoA persulfide (PDB: 2VIG), shown as blue sticks. In panels B and C, the sulfane sulfur in ^{201}Cys-SSH and in CoA-SSH persulfide are shown as yellow spheres.

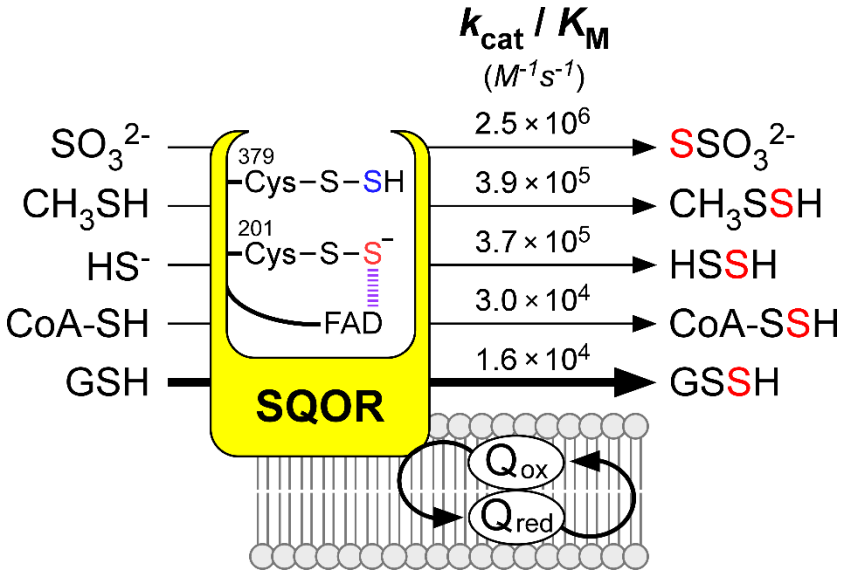

Figure 7. Catalytic promiscuity of the SQOR reaction. The catalytic efficiencies denoted for small thiophilic acceptors are derived from the most recent kinetic characterizations using SQOR embedded in nanodiscs (Refs. 54, 73, 93). In the CT complex intermediate, the sulfur derived from the active site cysteine trisulfide is shown in red, and the sulfur derived from H_2S is shown in blue.

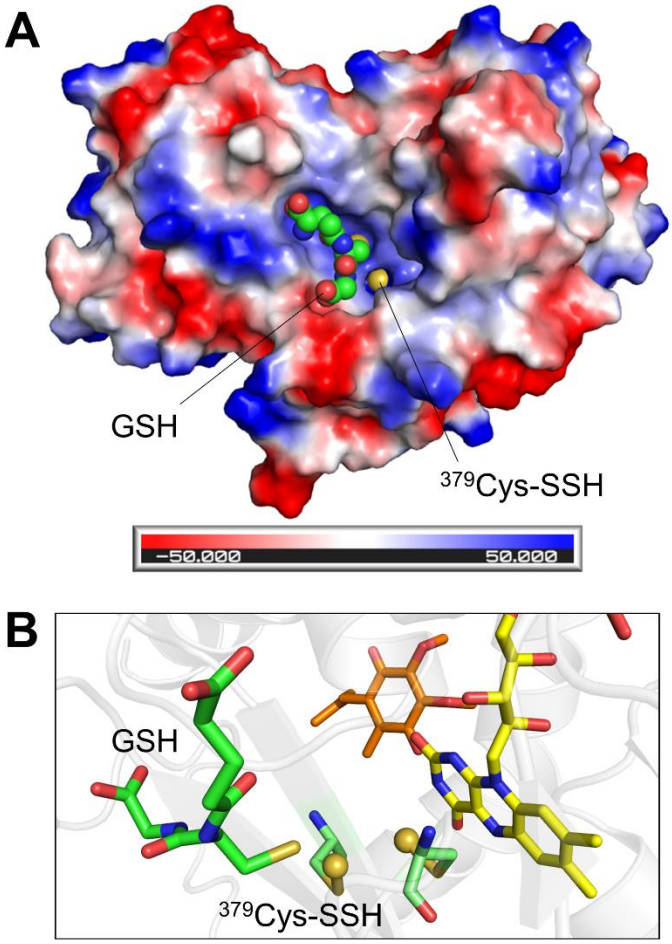

Figure 8. Structural basis for catalytic promiscuity in SQOR. A, Electrostatic surface potential map of the SQOR monomer, revealing a large electropositive cavity containing the exposed ^{379}Cys-SSH persulfide, shown as a yellow sphere. GSH is docked in the cavity and shown as green spheres. **B**, Orientation of the docked GSH, shown as green sticks, relative to the active site cysteine persulfides, shown as pale green sticks with the persulfide sulfurs shown as yellow spheres. The thiol moiety of GSH is oriented proximal to ^{379}Cys-SSH, which would facilitate sulfur transfer (PDB: 6OIB).

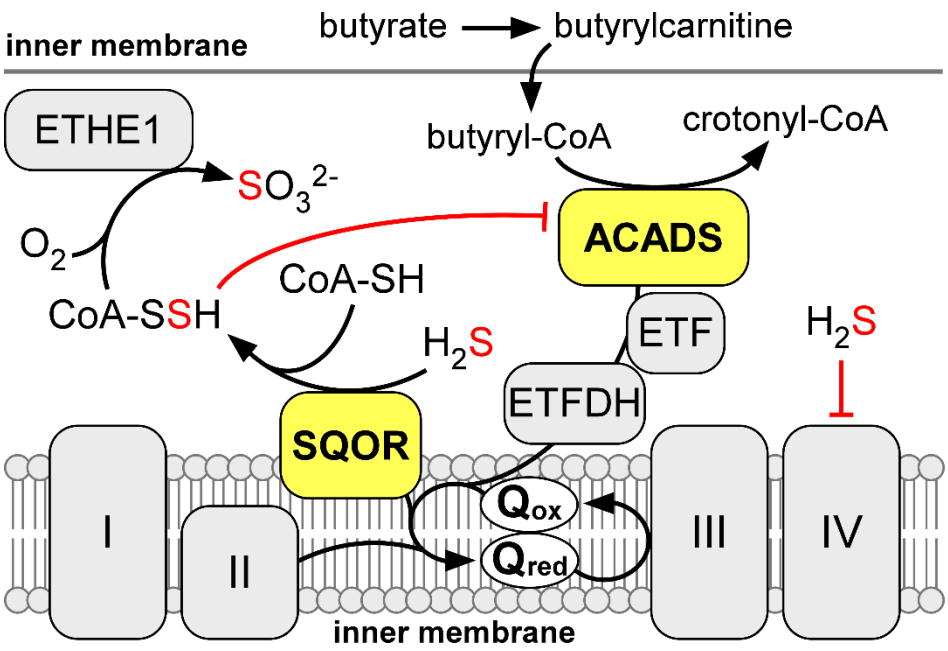

Figure 9. Interplay of sulfide and butyrate oxidation. The activities of SQOR and ACADS both drive electrons into the mitochondrial Q pool, which restricts the capacity of sulfide oxidation during acute H_2S exposures. As a countermeasure, SQOR can catalyze the formation of CoA-SSH, a tight-binding inhibitor of ACADs. Inhibition of ACADS by CoA-SSH relieves competition for the Q pool to prioritize sulfide oxidation.

Table of Contents Entry

Regulating sulfide toxicity and signaling: Utilizing an active site cysteine trisulfide, human sulfide quinone oxidoreductase detoxifies hydrogen sulfide, a respiratory poison. Herein, we detail the remarkable enzymology of sulfide quinone oxidoreductase and its potential modulation of sulfide signaling.

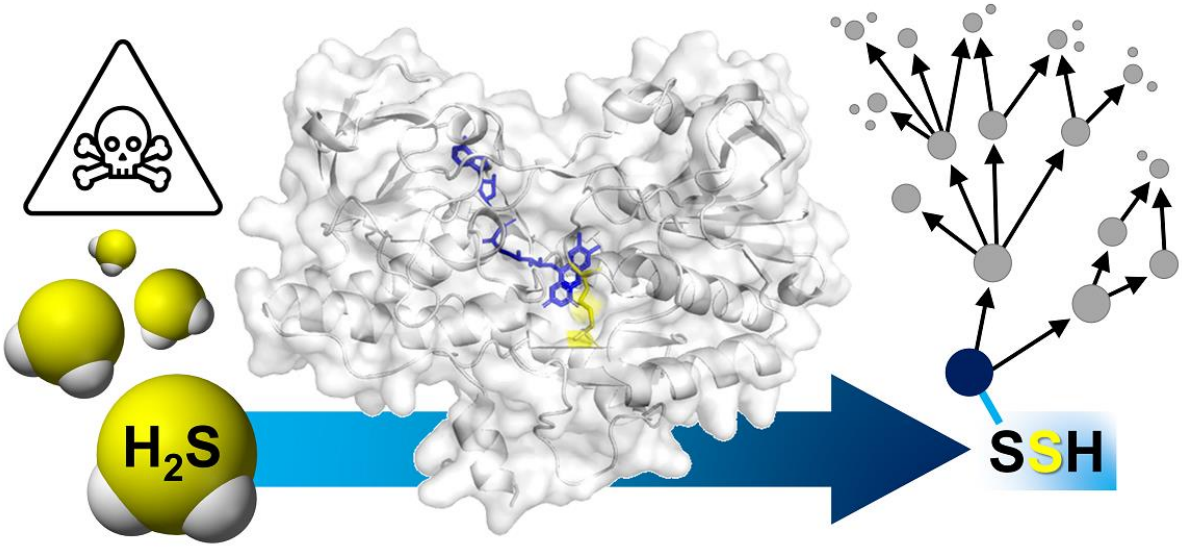

Keywords
protein structure, sulfide, flavin, redox chemistry, metabolism

Short Biographies for Authors

Aaron P. Landry obtained his BS and PhD degrees in Biochemistry at the Louisiana State University in Baton Rouge, LA. He is currently a postdoctoral fellow in Ruma Banerjee's group in the Department of Biological Chemistry at the University of Michigan. His research interests are focused on protein structure and function as they relate to the etiology and treatment of human diseases.

David P. Ballou obtained his BS in Chemistry with a minor in Music at Antioch College in 1965, and his PhD in Biological Chemistry from the University of Michigan in 1971 with Graham Palmer as supervisor. He carried out postdoctoral work with Vincent Massey and Minor Coon. He is an active Professor Emeritus of Biological Chemistry at the University of Michigan. His work has involved mechanistic and structural studies of enzymes involved in oxidative processes, especially flavin and iron containing enzymes that react with oxygen. He is known for his development of instrumentation for the study of rapid kinetics.

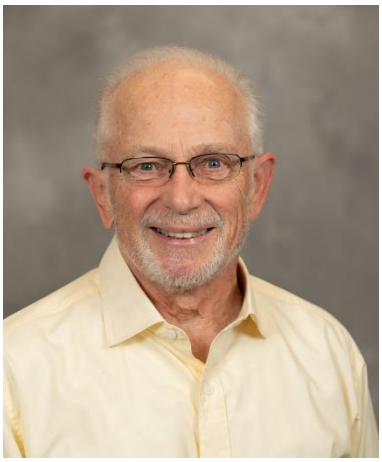

Ruma Banerjee obtained her BS and MS degrees in Botany at Delhi University and her PhD in Biochemistry at RPI, NY. Following postdoctoral research at the University of Michigan in Rowena Matthews' group, Ruma started her independent career at the University of Nebraska, where she was the founding director of the NIH-funded Redox Biology Center. In 2007, she moved back to the University of Michigan as the Vincent Massey Collegiate Professor of Biological Chemistry. Her research interests are focused on the chemical biology of H_2S and on vitamin B_{12} trafficking.